International Journal of Thin Films Science and Technology

http://dx.doi.org/10.12785/ijtfst/040314

Characteristics of Sb_2S_3 Thin Films Deposited by a Chemical Method

P. A. Chate[1,*] and *S. D. Lakde*[2,3].

[1]Department of Chemistry, J.S.M. College, Alibag. M.S. India.
[2]JJT University, Jhunjhunu, Rajasthan, India.
[3]Bhausaheb Nene College, Pen, (M.S.). India.

Received: 27 Jun. 2015, Revised: 22 Jul. 2015, Accepted: 24 Jul.2015.
Published online: 1 Sep. 2015.

Abstract: In the present paper, we have reported the room temperature growth of antimony sulphide (Sb_2S_3) thin films by dip method and detailed characterization of these films. The films were deposited from a reaction bath containing antimony chloride, glycine and sodium thiosulphate. We have analyzed the structure, morphology, composition, optical and electrical properties of Sb_2S_3 thin films. X-ray diffraction pattern showed that the films were polycrystalline. From optical absorption spectra the band gap of the material is estimated to be 2.27 eV. The electrical conductivity is of the order of 10^{-7} $(\Omega\ cm)^{-1}$. Composition analyses by EDAX show that the films are nearly stiochiometric in composition.

Keywords: Thin films; X-ray diffraction; Optical properties; Surface morphology.

1 Introduction

The semiconducting compounds are of great importance in electronic science in view of their photoconductivity, photoresistivity and thermoelectric power [1-2].

As an important V-VI group binary chalcogenide, antimony trisulfide with an energy band gap varying between 1.5 and 2.2 eV has attracted particular attention, owing to its good photovoltaic properties, high thermoelectric power, broad spectrum response, and suitable valence band position [3-5]. Some physical properties like photoelectric properties and the conduction and charge carrier transport mechanism have been reported in literature. [6-8]. It has special properties such as high refractive index, well defined quantum size effects [9-11] It is a n-type semiconductor [12].

This material has been applied in various areas such as television cameras with photoconducting targets, thermoelectric cooling devices, electronic and optoelectronic devices, solar energy conversion, visible light-responsive photocatalysis, microwave, switching devices, photovoltaic structures, resonant laser cavity and optical data storage devices [13-26]. It has been demonstrated that the properties of antimony trisulfide are determined predominantly by their crystal structure, size, and morphology. Therefore, the synthesis of Sb_2S_3 materials with well-controlled size and shape is of great significance for their applications. Up to date, a variety of 1D nanostructures of Sb_2S_3 such as nanorods [27-30], nanowires [31], nanotubes [32-33], and nanoribbons [34] have already been synthesized by various methods. Several investigators have prepared Sb_2S_3 thin films with different chemical methods such as spray pyrolysis [35-36], chemical bath deposition [37-38], successive ionic layer adsorption and reaction method [39], electrodeposition [40], dip and dry method [41] and vacuum evaporation [42-43]. The dip method for formation of thin films from aqueous solution is a promising technique because of its simplicity and economics. The starting chemicals are universally available and inexpensive. This method can be used to deposit films at low temperature which avoids oxidation of the deposited material. The deposition conditions are easily controlled to get improved orientation and grain structure of the film. The dip method has the major advantage with respect to other methods is that the films on different kinds of substrate shapes, and sizes can be deposited. Considering the technical importance of this material, fabrication of Sb_2S_3 with some inspired structures such as a flower-like structure by a convenient and efficient method has always been a great interest.

We report synthesis of Sb_2S_3 thin film by dip method. The deposited film samples were characterized by various techniques such as X-ray diffraction, scanning electron micrograph, EDAX. Optical and electrical properties are also studied.

2 Experimental Details

*Corresponding author E-mail: pachate04@rediffmail.com

The substrates used for depositing the films were non-conducting glass slides of the size 75 x 25 x 2 mm. All the chemicals used for the deposition were of AR grade. All the solutions were prepared in double distilled water. The chemicals used were antimony chloride, glycine, and sodium thiosulphate.

To prepare the bath, 10mL (0.2M) $SbCl_3$ was poured in 100mL beaker; other chemicals were used in the following sequence: 4mL (1M) glycine, 15mL (0.2M) sodium thiosulphate. The pH of the reactive mixture is 4.35. The total volume was made 50 mL with double distilled water. The temperature of the bath was maintained at 278 K using ice bath. The solution was stirred vigorously before dipping non-conducting glass substrates. The substrates kept vertically slightly tilted in a reactive bath. The temperature of the bath was then allowed to increases up to 298 K very slowly. The film was deposited on both sides of slides. After 5 hours, the slides were removed washed several times with double distilled water. The film was dried naturally and preserved in dark desiccators over anhydrous $CaCl_2$.

The film thickness was measured by weight difference method by using relation

$$t = m/\rho A \quad (1)$$

Where, m is the mass of the film deposited on the substrate, A is the area of the deposited films and ρ is the density of deposited material (Sb_2S_3 = 4.64 g/cm^3). The terminal thickness was found to be 0.71μm.

3 Result and Discussions

3.1 Growth mechanism

The deposition process of Sb_2S_3 is based on the slow release of $Sb^{+3}$and S^{-2} ions in the solution which then condenses ion by ion basis on the substrates. Deposition of Sb_2S_3 thin film occurs when the ionic product of Sb^{+3} and S^{-2} ions exceeds the solubility product of Sb_2S_3. [K_{sp} = 1.5 x10^{-93}] [44]. The concentration of Sb^{+3} and S^{-2} ions in the solution controls the rate of Sb_2S_3 formation. The rate of Sb^{+3} ions is controlled by glycine, which forms a complex $Sb[(Gly)_n]^{+3}$ with Sb^{+3}. The reaction for the formation of Bi_2S_3 thin films can be written as follows;

$$Sb[(Gly)_n]^{+3} \rightarrow Sb^{+3} + n\,(Gly)$$

$$Na_2S_2O_3 \rightarrow 2Na^+ + S_2O_3^{-2}$$

$$6S_2O_3^{-2} \rightarrow 3S_4O_6^{-2} + 6e^-$$

In acidic medium dissociation of $S_2O_3^{-2}$ take place as

$$3S_2O_3^{-2} + H^+ \rightarrow 3HSO_3^- + 3S$$

$$3S + 6e^- \rightarrow 3S^{-2}$$

$$2Sb^{+3} + 3S^{-2} \rightarrow Sb_2S_3$$

Deposition begins only when the chalcogenide concentration is high enough to allow nucleation to start, which occurs in the linear region of growth. As the limiting reactant is used up, growth will start slow down and eventually stop due to depletion of the reactant [45-46].

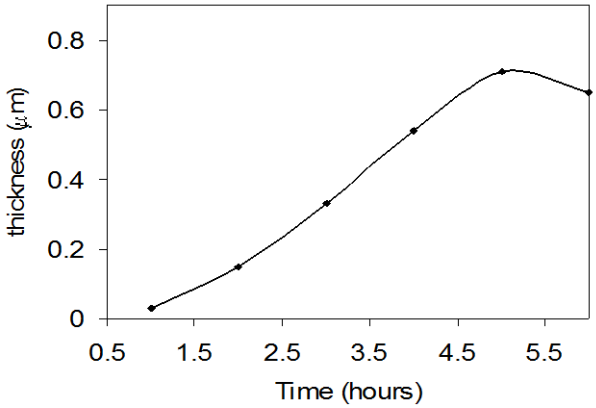

Fig. 1: Plot of thickness against deposited time.

The behaviour of thickness versus deposition time is showin in Fig.1. The film thickness increases with immersion time, but after 5 h the growth process reaches the saturation and further only lower thickness value can be achieved. This is mainly due to decrease in concentration of reactant with time as well as dissolution of the film in the solution. The deposited films are orange and transparent.

3.2 Structural characterization

Fig. 2 shows the x-ray diffractrogram of the Sb_2S_3 thin films. The broad hump in the diffractrogram is due to glass substrate as well as some amorphous phase of the sample. The film is crystallized in the orthorhombic phase and presents a preferential orientation along (101) plane.

Table 1: Comparison of standard and observed d values of Sb_2S_3 films.

Standard d value (Å)	Observed d value (Å)	Reflection plane
3.632	3.634	101
3.556	3.549	310
3.128	3.123	230
3.053	3.051	211
2.764	2.767	221
2.202	2.200	510
1.940	1.942	431
1.729	1.729	351

The (310) (230) (211) (221) (510) (431) (351) peaks were also observed at 2θ = 25.07, 28.55, 29.24, 32.32, 40.98, 46.74 and 52.91^0 respectively but these peaks are much lower intensity then the intensity corresponding reflection (101) plane (2θ = 24.47) The observed 'd' values, are compared with the standard data (JCPDS-6-0474) and shown in Table 1.

A method that evaluates the magnitude of the preferred orientation factor 'f' for a given plane (peak) relative to other planes (peaks) in material was employed

[47]. According to this method the preferred orientation factor 'f' (101) of the (101) plane for the Sb_2S_3 thin films has been calculated by evaluating the fraction of (101) plane intensity over the sum of intensities of all other peaks has been evaluated for the films.

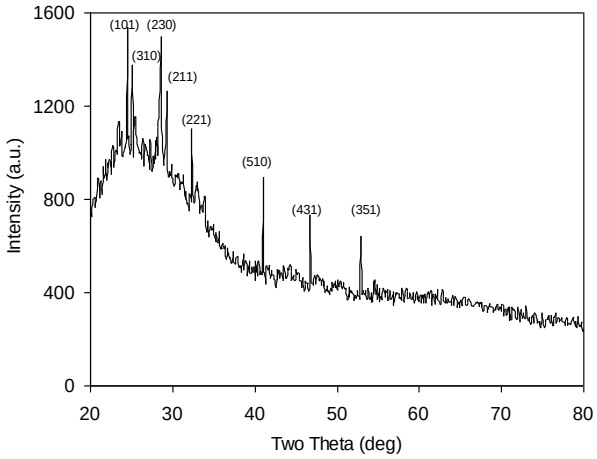

Fig. 2: X-ray diffraction of Sb_2S_3 thin films.

f(101) = 0.1699, f(310) = 0.1519, f(230) = 0.1654, f(211) = 0.1398, f(221) = 0.1218, f(510) = 0.0988, f(431) = 0.0810, f(351) = 0.0710. The lattice constant a, b, and c are calculated using the following relation.

$$(1/d^2) = (h^2/a^2+k^2/b^2+l^2/c^2) \quad (2)$$

The lattice parameters was found to be a =11.225, b =11.202 and c =3.840 Å, which are in good agreement with the standard value [48]. The unit cell volume can be calculated by using equation: [49]

$$V= abc \quad (3)$$

The unit cell volume was found to be 482.85 $(Å)^3$ The crystallite size is calculated from the diffraction peak broadening from the line (101) by using Scherrer relation; [50]

$$D = 0.9\lambda /\beta\cos\theta \quad (4)$$

The crystallite size was found to be 150.56nm. The microstrain (ε) developed in the films were calculated by using equation [51]

$$\varepsilon = \beta\cos\theta/4 \quad (5)$$

The value was found to be 2.302 x 10^{-4}. Dislocation density is calculated using the relation [52]

$$\delta = n/D^2 \quad (6)$$

Where n is the factor which is equal to unity for minimum dislocation density. The value was found to be 4.411x 10^{13} m^{-2}.

3.3 Morphological and compositional Study

The scanning electron micrograph of Sb_2S_3 thin film is shown in Fig. 3. Spherical and bunches of thread like structure was observed. The spherical grains are fused with each other. It well covers the glass substrates. The threads are randomly distributed.

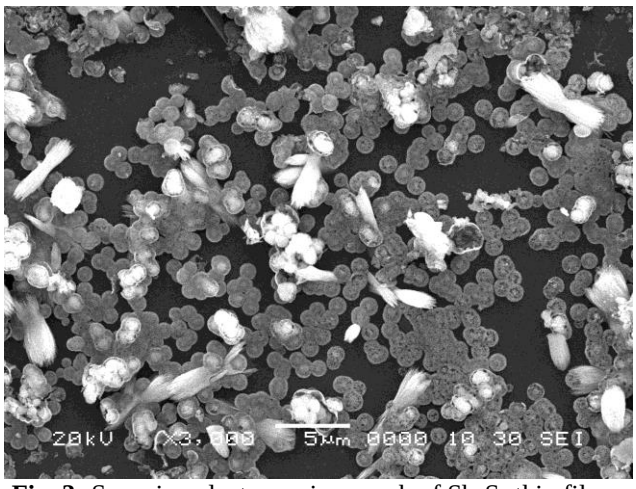

Fig. 3: Scanning electron micrograph of Sb_2S_3 thin films.

Quantitative analysis of the film was carried out using the EDAX technique for Sb_2S_3 to study the composition in the film.

Fig. 4 shows a typical EDAX pattern of Sb_2S_3 thin films. The elemental analysis was carried out only for Sb and S; the average atomic percentage of Sb: S was 46.22: 53.78, showing that the film is slightly rich in S^{-2} and well agree well with the result reported by Mane et al [53].

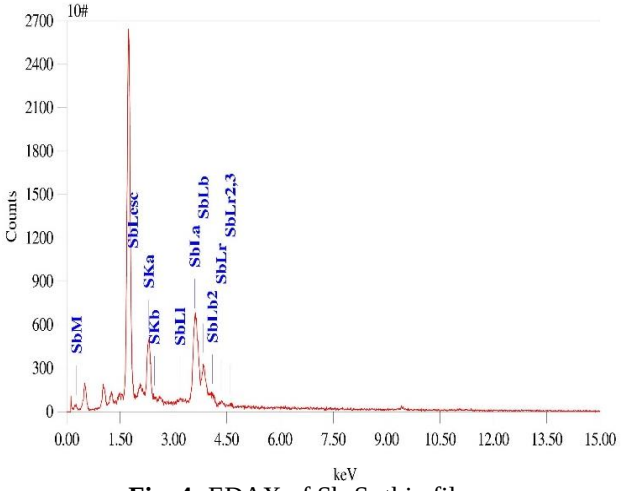

Fig. 4: EDAX of Sb_2S_3 thin films.

3.4 Optical Characterization

Fig. 5 shows the absorption spectra of Sb_2S_3 thin films in the wavelength range of 400-800 nm. The absorption spectra were used to calculate band gap, type of optical transition and absorption coefficient, etc. The study show that the presences of absorption edge of exponential shape. It is due to homogeneity of the films and normal band structure. The spectra shows two regions, one for higher wavelength with practically lower absorption and other for

lower wavelength in which absorption increases steeply. The optical studies revealed that the films are highly absorptive with direct type of transition. The values of the absorption coefficient, α, are in the order of 10^4 cm^{-1} in the investigation spectral range (At 400 nm α = 2.36 x 10^4, At 800 nm α = 0.91x 10^4).

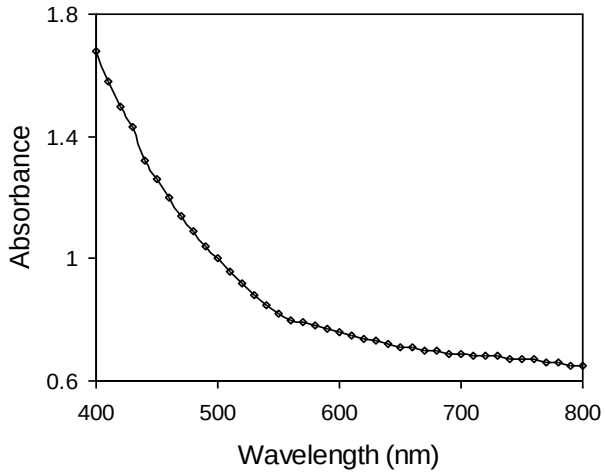

Fig. 5: Absorption spectrum of Sb_2S_3 thin films.

The fundamental absorption, which corresponds to electron excitation from the valence band to conduction band, can be used to determine the nature and the value of the optical band gap (Eg). The relation between the absorption coefficient, α, and the incident photon energy, hν, can be written as [54];

$$(\alpha h\nu)^n = A(h\nu - Eg) \quad (7)$$

Where A is a constant depending on the transition probability and n is an index that characterizes the optical process and is theoretically equal to 1/2, 2, 1/3 or 2/3 for indirect allowed, direct allowed, indirect forbidden and direct forbidden transition, respectively [55].

The usual method to calculate the band gap energy is to plot a graph between $(\alpha h\nu)^n$ and photon energy, hν, and find the value of n which gives the best linear graph. This value of n decides the nature of energy band gap or transition involved. If the appropriate value of n is used to obtain linear plot, the value of Eg will be given by intercept on the hν axis. To apply the relation (7) for Sb_2S_3 thin films the dependences $(\alpha h\nu)^{1/2}$ $(\alpha h\nu)^2$ $(\alpha h\nu)^{1/3}$ $(\alpha h\nu)^{2/3}$ versus hν were plotted. For Sb_2S_3 thin film, the best plot that covers the widest range of data and intercept the hν axis is obtained only for the $(\alpha h\nu)^2 = f(h\nu)$ dependences (Fig 6).

The obtained value n =2, characterizes a direct allowed optical transition which occur in polycrystalline films [56-57]. The value of direct band gap corresponding of polycrystalline Sb_2S_3 thin film was found to be 2.27 eV. This result is good agreement with the reported values in literature for Sb_2S_3 thin films prepared by different methods [58]. The value of n = 2 is confirmed by a plot of ln(hν-Eg)and ln(αhν). The slope of the line was nothing but the value of n. The slope of the graph was found to be 1.97 (Fig. 7).

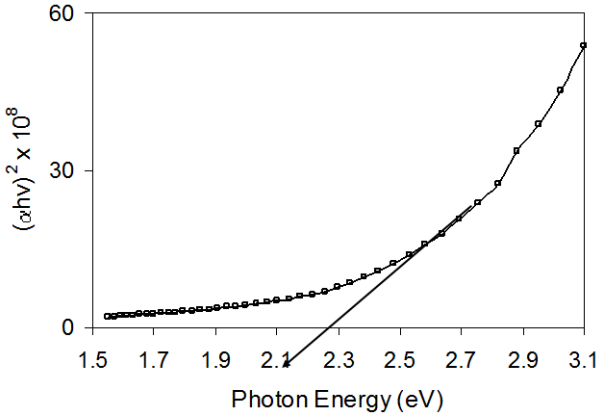

Fig. 6: Plot of $(\alpha h\nu)^2$ versus photon energy for Sb_2S_3 thin films.

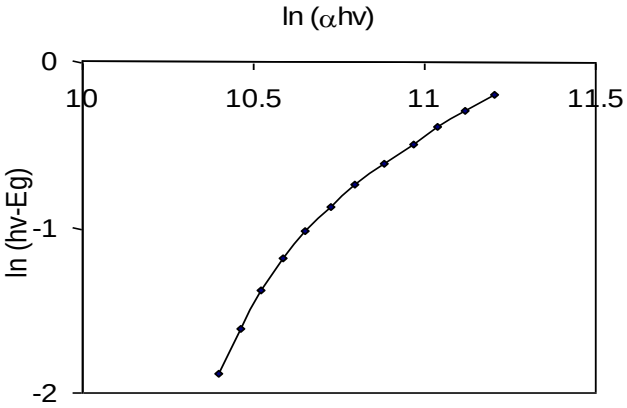

Fig. 7: Plot of ln (hν-Eg) versus ln (αhν) for Sb_2S_3 thin films

3.5 Electrical Properties

The dark electrical conductivity of as deposited Sb_2S_3 film on non-conducting glass slide was determined, in the temperature range 300-525K. At room temperature the specific conductance was found to be in the order of $10^{-7}(\Omega cm)^{-1}$, which agrees well with the earlier reported value [59]. The values of specific conductance at 300 and 525 K are reported in Table 2.

Table 2: Electrical properties of Sb_2S_3 thin films

	300K	525K
Specific Conductance $(\Omega cm)^{-1}$	1.516 x 10^{-7}	2.540 x 10^{-4}
Activation Energy (eV)	0.119 (LT)	0.209 (HT)

The low value of conductivity for as deposited film may be due to low crystallinity and small thickness of the film. The electrical properties of polycrystalline thin films are mainly depend upon their structural characteristics and composition [60-61]. A plot of log (conductivity) versus inverse absolute temperature for the cooling curve is shown

in the Fig. 8. A plot shows that electrical conductivity has two linear regions, the low temperature extrinsic and high temperature intrinsic regions, indicating the presence of two conduction mechanism. The high temperature region is due to grain boundary scattering limited conduction mechanism, while a low temperature region is due to variable range hopping conduction mechanism. The activation energy is calculated using exponential form of Arrehenius equation. In the present case the activation energies were in the range of 0.119-0.209 eV. They are consistent with previously observed values [62].

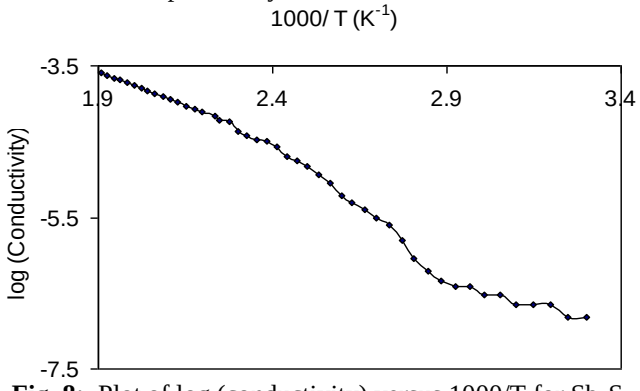

Fig. 8: Plot of log (conductivity) versus 1000/T for Sb_2S_3 thin films.

Since; the temperature activation energy represents a mean value of the inter-crystalline barrier height combining the effects of both carrier concentration and mobility, it is expected that measured values will differ between workers using different preparation conditions. However, the general dependence of conductivity on temperature is clearly consistent, and indicates the existence of a well-defined potential barrier between inter-crystalline grains; which may be overcome by thermal activation.

4 Conclusions

1) Sb_2S_3 can be deposited at room temperature by chemical method.
2) The film formation takes place via nucleation and growth.
3) Films were orange, polycrystalline in orthorhombic structure.
4) Optical studies revealed direct band gap of 2.27 eV.
5) The conductivity of the films are in the order of $10^{-7}(\Omega\ cm)^{-1}$

References

[1] S.R. Gadakh, C.H.Bhosale, *Mater. Chem. Phys*.78 (2002) 367.

[2] G. Ghosh, B.P.Verma, *Thin Solid Films* 60 (1979) 61.

[3] X. Shuai, W. Shen, *Nanoscale Res. Lett.* 7 (2012) 199.

[4] S. Ibuke, S. Yochimatsu, *J. Phys. Soc. Jpn* 10 (1955) 549,

[5] K. Li, F. Huang, X. Lin, *Scripta Mater.* 58 (2008) 834.

[6] Mary. J. Chockalingam, K. Nagaraja Rao, N. Rangarajan, C.V. Suryanarayana, *J. Phys. D: Appl. Phys.* 3 (1970) 1641.

[7] E. Montrimas, A. Pazera, *Thin Solid Films* 34 (1976) 65.

[8] N. Mathew, R.Oommen, U. Rajalakshmi, *Chalcogen. Lett.* 7 (2010) 701.

[9] C. Lokhande, B. Sankapal, R. Mane, H. Pathan, M. Muller, M. Giersig, V.

Ganesan, *Appl. Surf. Sci*. 193 (2002) 1.

[10] A.Salem, M. Selim, *J. Phys. D Appl. Phys.* 34 (2001) 12

[11] B. Krishnan, A. Arato, E. Cardenas, T. Roy, G. Castillo *Appl. Surf. Sci.* 254, (2008) 3200.

[12] K.Y. Rajpure, C.H. Bhosale, *Mater. Chem. Phys.* 64 (2000) 14.

[13] D. Arivuoli, F. Gnanam, P. Ramasamy, *J Mater Sci. Lett* 7 (1988) 711.

[14] O. Savadogo, K. Mandal, *SolEner. Mater Sol. Cells* 26 (1992) 117.

[15] Q. Han, L. Chen, M. Wang, X. Yang, L. Lu, X. Wang, *Mater Sci Eng. B* 166

(2010) 118.

[16] M. Sun, D. Li, W. Li, Y. Chen, Z. Chen, Y. He, X. Fu, *J Phys Chem C* 112, (2008) 18076.

[17] X. Cao, L. Gu, L. Zhuge, W. Gao, W. Wang, S. Wu, *Adv. Funct. Mater.* 16, (2006) 896.

[18] I. Zawawi, A. Moez, F. Terra, M. Mounir, *Thin Solid Films* 324(1998) 300.

[19] N. Mathew, R.Oommen, U. Rajalakshmi, C. Sanjeeviraja, *Chalcogen. Lett.* 8, (2011) 441.

[20] S. Messina, M. Nair, P.Nair, *Thin Solid Films*. 515 (2007) 5777.

[21] Y. Lazcano, M. Nair, P.Nair, *J. Electrochem. Soc*152 (2005) 635.

[22] R.S. Mane, C.D. Lokhande, *Mater. Chem. Phys.* 78 (2003) 385.

[23] O. Savadogo, *Sol. Ener. Mater. Sol. Cells*. 52 (1998) 361.

[24] E. Perales, G. Lifante, F. Rueda, C. Hares, *J. Phys. D: Appl. Phys*. 40 (2007), 2440.

[25] E. Perales, F. Rueda, J. Lamela, C. Heras, *J. Phys. D: Appl. Phys.* 41 (2008), 45403.

[26] P. Arun, A. Vedeshwar, N. Mehra, *Mater. Res. Bull.* 32 (1997) 907.

[27] J. Ota, S. Srivastava, J. *CrystGrowth* 7 (2007)343.

[28] P. Estevané, M. Sánchez, *Mater Lett* 64 (2010) 2627.

[29] J. Ota, P. Roy, S. Srivastava, B. Nayak, A. Saxena, *J. Cryst Growth* 8 (2008) 2019.

[30] A. Alemi, S. Joo, Y. Hanifehpour, A. Khandar, A. Morsali, B. Min *J Nanomater* 10 (2011) 528.

[31] Z. Geng, M. Wang, G. Yue, P. Yan . *J Cryst Growth* 310 (2008) 341

[32] J. Yang, Y. Liu Y, H. Lin, C. Chen, Adv *Mater.* 16 (2004) 713.

[33] X. Cao, L. Gu, W. Wang, W. Gao, J. Zhuge, Y. Li *J Cryst Growth* 286 (2006) 96.

[34] Y. Yu, R. Wang, Q. Chen, L. Peng, *J PhysChem B* 110 (2006)13415

[35] C. Bhosale, M. Uplane, P. Patil, C. Lokhande, *Thin Solid Films* 248(1994) 137.

[36] V. Killedar, C. Lokhande, C. Bhosale, *Mater. Chem. Phys.* 47 (1997) 104

[37] R.Mane, B. Sankpal, C. Lokhande, *Thin Solid Films*353 **(**1999) 29.

[38] J. Desai, C.D. Lokhande, *Thin Solid Films* 237 (1994) 29.

[39] B. Sankpal, H. Pathan, C. Lokhande, *J. Mater. Sci. Lett.* 18 (1999) 1453.

[40] N.Yesugade, C. Lokhande, C. Bhosale, *Thin Solid Films* 263 **(**1995) 145.

[41] B.Nayak, H.Acharya, T. Choudhuri, G. Mitra, *Thin Solid Films* 92 (1982) 309.

[42] N. Tigau, C. Gheorgies, G. Rusu, S. Bota, *J. Non-Cryst. Solids* 351(2005) 987.

[43] N. Tigau, *Cryst. Res. Technol*. 42 (2007) 281.

[44] R. Weast, *CRC Handbook of Chem. Phys. 69 edition. Boca Raton: CRC Press*; 1988.

[45] G. Godes, *Chemical Solutions Depoition of Semiconductor Films, Marcel Dekker*, 2003.

[46] H.E. Esparza-Ponce, J. Hernandez-Borja, A. Reyes-Rojas, M.Cervantes- Sanchez,Y.V.Vorobiev, R.Ramirez-Bon, J.F.Perez-Robles, J. Gonalez- Hernandez, *Mater. Chem.Phys*. 113 (2009) 824.

[47] S. Prabahar, M. Dhanam*J. Cry. Growth* 285(2005) 41.

[48] J. Desai, C.D. Lokhande, *J. Non-Crystalline Solids* 181 (1995) 70.

[49] P. Kumar, N. Jain, R. Agarwal *Chalcogen. Lett.*7 (2010) 89.

[50] P. A. Chate, D. J. Sathe, P. P. Hankare, U. B. Sankpal*J Mater Sci: Mater Electron*24 (2013) 2000.

[51] P.A. Chate, S.S. Patil, J.S. Patil, D.J. Sathe, P.P. Hankare, *Physica B* 411 (2013) 118.

[52] D. Richards, R. Angelis, M. Kramer J. House, D. Cunard, D.Shea, *Adv. X-ray Analysis*, 47 (2004) 354.

[53] R.S.Mane, C.D.Lokhande, *Surf. Coat. Technol.* 172 (2003) 51.

[54] P.P. Hankare, P.A. Chate*Mater. Chem. Phys.* 117 (2009) 347.

[55] R. Smith, *Semiconductors, 2nd Edition, Cambridge University Press, Cambridge, NY*, 1978.

[56] N. Tiagu*Rom. J. Phys.* 53 (2008) 209.

[57] R. Krishan, A. Arato, F. Cardenas, T.Roy, G. Castillo, *Appl. Surf. Sci.* 254 (2008) 3200.

[58] F. Ezema, A. Ekwealor, P. Asogwa, P. Ugwuoke, C. Chigbo, R. Osuji, *Turk. J. Phys.* 31 (2007) 205.

[59] R.S.Mane, C.D.Lokhande, *Mater. Chem. Phys.* 82 (2003) 347.

[60] K.L.Chopra, *Thin Film Phenomenon (New York: McGraw-Hill)* 1969.

[61] G.I.Rusu, M.E.Popa, G.S.Rusu, I Salaoru, *Appl. Surf. Sci*., 218 (2003) 222.

[62] K.Y. Rajpure, A.L.Dhebe, C.D. Lokhande, C.H.Bhosale, *Mater. Chem. Phys.* 56 (1998) 177.